Theoretical and experimental investigations of high-power self-mode-locked Pr:YLF visible lasers

SAIYU LUO, BIN XU, HUIYING XU, AND ZHIPING CAI [1,*]

[1] *Department of Electronic Engineering, Xiamen University, Xiamen 361005, China*
**opex@osa.org*

Abstract: We demonstrate efficient self-mode-locked green and red lasers with repetition rate of tens and hundreds of MHz in a Pr:YLF crystal. Using double-end blue-diode-pumped geometry, more than 0.68 W average output power at 522 nm and more than 1.44 W at 639 nm are obtained, which are believed to be the highest average output power for mode locked lasers operating in visible wavelength region. Mechanism of the self-mode-locked Pr:YLF visible lasers is also analyzed theoretically.

OCIS codes: (140.3580) Lasers, solid-state; (140.3480) Lasers, diode-pumped; (140.4050) Mode-locked lasers; (140.7300) Visible lasers; (190.3270) Kerr effect.

References and links (see Section 4)

1. S. Engler, R. Ramsayer, and R. Poprawe, "Process Studies on Laser Welding of Copper with Brilliant Green and Infrared Lasers," Phys. Procedia **12**, 339(2011).
2. S. Ruan, B. H. T. Chai, J. M. Sutherland, P. M. W. French, and J. R. Taylor, "Kerr-lens mode-locked visible transitions of a Pr:YLF laser," Opt. Lett. **20**, 1041-1043 (1995).
3. Y. P. Tong, A. V. Shestakov, B. H. T. Chai, J. M. Sutherland, P. M. W. French, and J. R. Taylor, "Self-starting Kerr-lens mode-locked femtosecond Cr4+:YAG and picosecond Pr^{3+}:YLF solid-state lasers," Opt. Lett. **21**, 644-646 (1996).
4. M. Gaponenko, P. W. Metz, A. Härkönen, A. Heuer, T. Leinonen, M. Guina, T. Südmeyer, G. Huber, and C. Kränkel, "SESAM mode-locked red praseodymium laser," Opt. Lett. 39(24), 6939 (2014).
5. Y. X. Zhang, H. H. Yu, H. J. Zhang, A. D. Lieto, M. R. Tonelli, and J. Y. Wang, "Laser-diode pumped self-mode-locked praseodymium visible lasers with multi-gigahertz repetition rate," Opt. Lett. **41**(12), 2692(2016).
6. Y. X. Zhang, H. H. Yu, R. Zhang, G. Zhao, H. J. Zhang, Y. X. Chen, L. M. Mei, M. R. Tonelli, and J. Y. Wang, "Broadband atomic-layer MoS2 optical modulators for ultrafast pulse generations in the visible range". Opt. Lett. **42**(3), 547 (2017).
7. K. Iijima, R. Kariyama, H. Tanaka, and F. Kannari, "Pr^{3+}:YLF mode-locked laser at 640 nm directly pumped by InGaN-diode lasers," Applied Optics **55**(28), 7782 (2016).
8. L. Q. Song, Z. L. Xi, Z. X. He, D. Yuan, Y. Y. Ji, and J. G. Yong, "The effect of the depth of single longitudinal mode modulation in Q-switching pre-Pr^{3+}:YLF laser", Opt. Comm. **372**, 250-254 (2016).
9. Y. X. Bai, S. S. Chen, Z. J. Wang, and G. Q. Zhang. "Novel self-mode-locking mechanism in narrow-band lasers," Appl. Phys. Lett. **63**(19), 2597 (1993).
10. J. J. Sanchez-Mondragon and G. E. Torres-Cisneros, "Pulse compression caused by a spectral hole in an inhomogeneously broadened line of an amplifier," J. Opt. Sot. Am. B **4**(1), 64-71 (1987).

1. Introduction

Mode-locking is one of the primary methods to obtain ultra-short laser pulses. Ultra-short pulses in the visible spectral region have many applications in various fields, especially industry and scientific research. For instance, in industry, compared with continuous-wave lasers, ultra-short visible lasers have much higher pulse peak powers as they output their energies in a very short time, leading to a useful application of metal processing [1]. In scientific research, high quality lasers sources such as mode-locked lasers or single frequency lasers in the visible spectral region are always desirable since they can be used to explore the energy-level properties of other laser materials or generate efficient down-conversion laser emissions.

Mode locking in the visible spectral region has been first realized in the middle of 1990s. The first mode-locked Pr:YLF visible lasers at 607 and 639 nm utilizing the Kerr-lensing

effect and initiated by liquid saturable absorbers were realized in 1995 by introducing argon-ion lasers as the pump source [2]. For the two wavelengths, 18 mW and 34 mW was achieved with repetition rate of 125 MHz and pulse width of 9.7 ps and 8.5 ps, respectively, which is the shortest optical pulse in the visible spectral region. One year later, the first self-staring Kerr-lens mode locked laser at 607 nm with output power of 15 mW and pulses width of 15 ps was reported by using Pr:YLF as the gain media, which was also pumped by an argon-ion laser [3]. Almost ten years later, in 2014, with the help of highly efficient pump source, 2ω-OPSL, mode-locked Pr^{3+} solid-state laser at 640 nm was obtained by Gaponenko et al, with pulses duration of ~18 ps and repetition rate of 85.6 MHz, based on semiconductor saturable absorber mirror (SESAM) [4]. The maximum averaged output power was only about 16 mW at an incident pump power of 3.75 W. Recently, Zhang et al. reported self-mode-locked Pr:GLF lasers at green, orange, red and deep red with the repetition rates of 2.8 GHz, 3.1 GHz, 3.1 GHz, and 3.0 GHz, respectively [5]. For the red laser, the maximum output power reached 612 mW with the slope efficiency of 46.9% at 639 nm. The obtained pulse widths range from 53 ps to 74 ps, which were 5~7 times larger than previous work. Subsequently, researchers from the same group have reported passive mode-locking Pr:GLF lasers at 522, 608 and 639 nm with output powers of 10, 18 and 46 mW, respectively [6], with the help of two-dimensional photoelectric material MoS_2. The achieved pulse widths were 25-55 ps with repetition rates of ~100 MHz. In addition, recently, Iijima et al. reported mode-locked Pr:YLF laser at 640 nm with a maximum averaged output power of 65 mW and a pulse width of 45 ps at a pulse repetition rate of 108 MHz [7].

All in all, owing to residual absorption brought by the additionally introduced optical elements, passive-mode-locking based on SESAMs and saturable absorbers have the disadvantages that the average output powers are limited. In contrast, self-mode-locking operations could achieve larger average output powers without extra intracavity loss. In this work, we presented efficient diode double-end pumped SML lasers at 639 and 522 nm, the average output power reached 1.44 and 0.68 W, respectively, which is the highest in all the SML results in visible spectral region ever reported. Moreover, a detailed theoretical analysis was presented to explain the origin of SML.

2. Experimental Setup

Fig. 1 depicts the experimental setup for the self-mode-locked Pr:YLF red laser using a six-mirror long cavity with a double-end pumping scheme. The two pump sources were both commercially available blue diode lasers with maximum output power of about 1.8 W and emitting peak wavelength of around 444 nm. Two focusing lenses, both with 50 mm focal length, were used to inject the pump beam into the laser crystal from the two sides, with average pump sizes of approximately 65 μm.

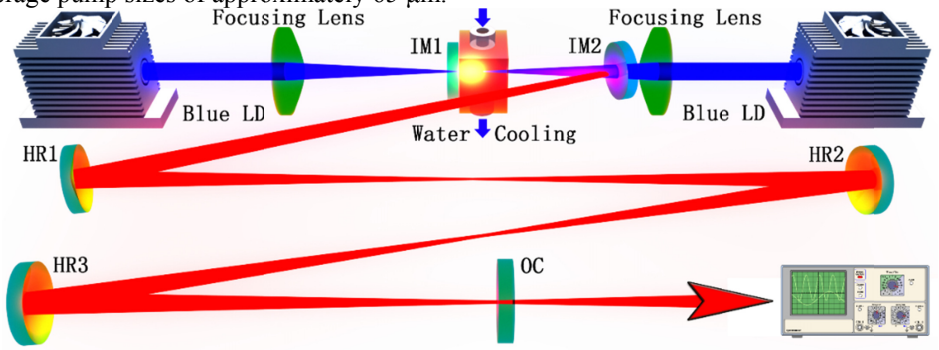

Fig. 1 Schematic of the self-mode-locked Pr:YLF red laser

For red self-mode-locking, a complex six-mirror and a relatively simple three-mirror cavity was used during the experiments. As shown in Fig. 1, for the six-mirror cavity, IM1

and IM2 have high transmission (>95%) at ~444 nm and high reflection (>99.9%) at 639 and 522 nm. HR1~HR3 are all concave mirrors with curvature radii of 300 mm and have high-reflection coating of >99.9% at 639 nm. The output coupler (OC) was a coated plane mirror with a transmission of 3.5% at 639 nm. The distance between IM1 and IM2 plus the distance between IM2 and HR1 equals ~300 mm. The distance between HR1 and HR2 and the distance between HR2 and HR3 were both around 600 mm. The distance between HR3 and OC was ~300 mm. Thus, the total cavity length was ~1.8 m.

A three-mirror cavity with a total length of about 0.3 m was also used to operate the red self-mode-locked Pr:YLF laser by removing the HR1-HR3 mirrors and at the same time replacing the OC with a curved one (300 mm of radius of curvature). The curved OC has a high-reflection coating of >99.9%. Hence, it needs to be mentioned here that the goal of this three-mirror cavity is just to confirm the self-mode-locked operation by altering the pulse repetition rate significantly. No suitable OC could be available during the experiments.

For the 522 nm laser, only three-mirror cavity was used. The two input mirrors IM1 and IM2 have high transmission (>95%) at pumping wavelength, high reflection (>99.9%) at 522 nm and high transmission (>60%) around 607 and 639 nm to suppress the high gain emissions at those wavelengths. The concave OC has a radius of curvature of 300 mm and transmission of 1.9% at 522 nm.

The active medium was an *a*-cut and 0.2 at. % doped Pr:YLF crystal with a length of ~8 mm. Both end faces of the Pr:YLF crystal were polished and uncoated. The laser crystal was wrapped with indium foil to improve the thermal contact and mounted in a water-cooled copper holder. The water temperature was maintained around 18°C to eliminate thermal effect.

3. Results and discussion

Laser output powers for the two wavelengths are first reported in Fig. 2. For the six-mirror 1.8-m long cavity operating at 639 nm, a maximum average output power of about 1.44 W was extracted with a total laser slop efficiency of about 57.3% with respect to the absorbed pump power. For the three-mirror green self-mode-locked laser, a maximum average output power up to 0.68 W was obtained with slop efficiency of about 29.9%.

It should be pointed out that the pump power was injected into the laser crystal one by one. That is to say, the left-side pump source was first used with output power increasing from zero to maximum, and then the right-side pump source was started. This could explain the output power characteristics of the red and green laser, as shown in Fig. 2 that there are slow increasing areas starting from about 1.4 W of absorbed pump power, which corresponded to the start-up of the right-side pump source. In fact, the introduction of the right-side pump source increased the pump power absolutely, but also increased the pump volume inside the laser crystal. As a result, it led to the decrease of average pump intensity, and therefore the standstill of the output power.

The self-mode-locked 639 nm laser spectrum is shown in Fig. 3, registered by Hewlett Packard 8560E Series Optical Spectrum Analyzer with a resolution of 0.08 nm under maximum pump power. The center wavelength was 639.4 nm, and the spectral width (FWHM) was measured to be 0.39 nm.

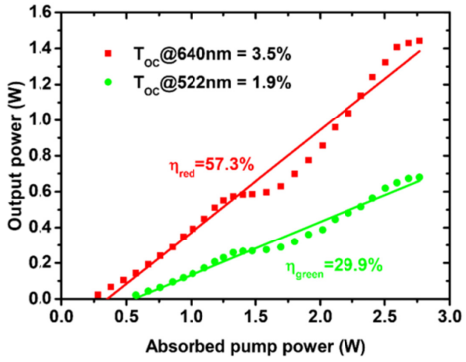

Fig. 2 Self-mode-locked laser performance of the ~1.8 m cavity 639 nm (red) and ~0.3 m 522 nm (green) laser operations.

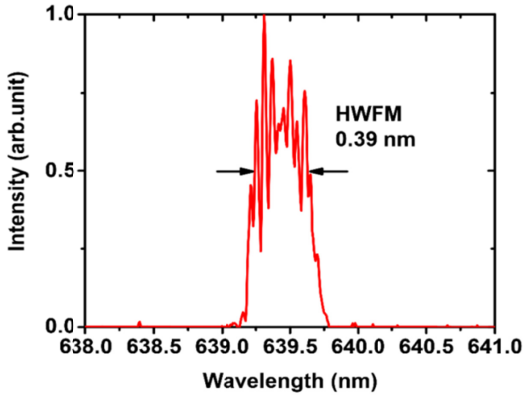

Fig. 3. Optical spectrum of the self-mode-locked Pr:YLF laser for 639 nm at cavity length of ~1.8 m measured at the maximum pump power.

The mode-locked pulses trains were detected by a free space high sensitivity PIN photo detector unit (Menlo Systems, Inc. FPD310-FV with rise time 0.7 ns), whose output signal was connected to a digital mixed signal oscilloscope (Tektronix MSO 3054) with 500 MHz electrical bandwidth and a sampling interval of 0.4 ns. Fig. 4 shows the measured pulse train for the self-mode-locking operated at the wavelength of 639 and 522 nm. The figures on the left side of Fig. 4, i.e. Fig. 4 (a-c), are the ones with time span of 200 ns, and the figures on the right side of Fig. 4 are the ones with time span of 40 μs. The stable mode-lock oscillation could be maintained for several hours during the laser experiments.

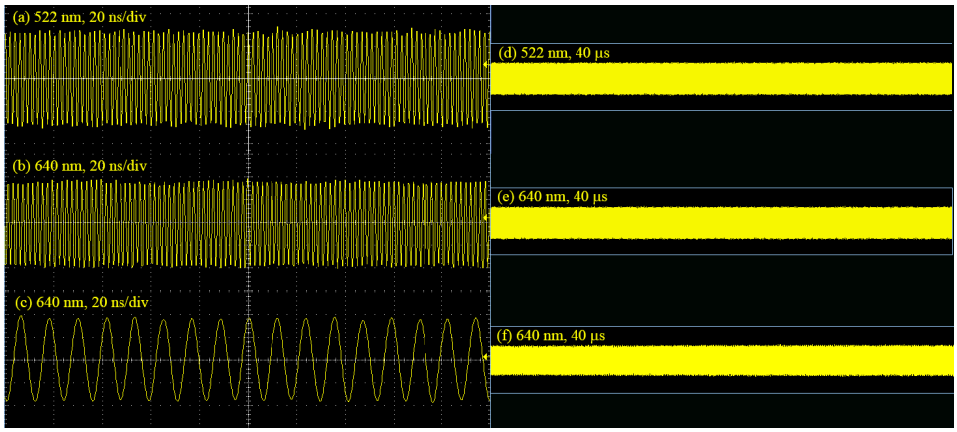

Fig. 4 Output pulse trains of the self-mode-locked lasers operating at the wavelength of 639 and 522 nm with a cavity length of ~0.3 m ((a), (b), (d), (e)) and ~1.8 m ((c), (f)) in time span of 200 ns ((a), (b), (c)) and 40 µs ((d), (e), (f)).

The radio-frequency (RF) spectra of the mode-locking outputs are shown in Fig. 5, using RF spectrum analyzer (GωINSTEK, GSP-930) with a bandwidth of 3.0 GHz. As depicted in Fig. 5(a) and (b), fundamental beat notes of 495 and 493 MHz were registered for the three-mirror cavity operating at 522 and 639 nm, indicating effective cavity lengths of about 303 and 304 mm when the cavities were optimized for the maximum output power. Fig. 3(c) shows the fundamental beat note of 83 MHz for the six-mirror cavity operating at 639 nm, corresponding to a cavity length of about 1805 mm. The detail of the fundamental beat notes are shown in Fig. 6 with RBW of 10 Hz. For the 522 nm green laser, as Fig. 6 (a) shown, the extinction ratio is about 49 dBm. For the 639 nm red laser, the extinction ratios are better than 48 and 55 dBm, respectively for the 0.3 m (Fig. 6(b)) and 1.8 m (Fig. 6(c)) laser cavities. The high contrast and the absence of modulations in the wide span are evidences of a very stable and clean mode-locked operation of the Pr:YLF oscillator.

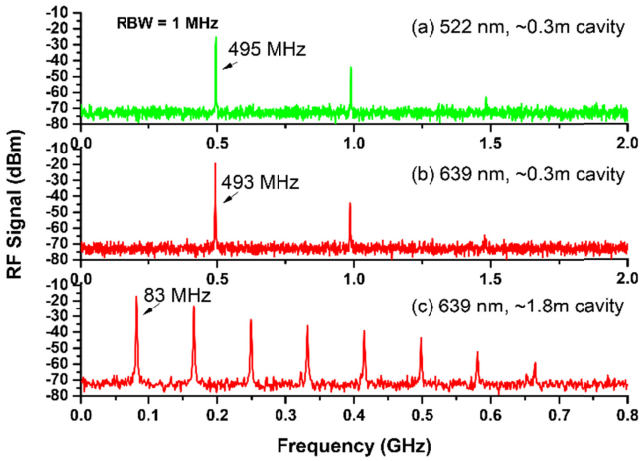

Fig. 5 Radio-frequency spectra of the self-mode-locked lasers operating at the wavelength of 522 nm and 639 nm with a cavity length of ~0.3 m ((a), (b)) and ~1.8 m ((c)) at a resolution of 1 MHz.

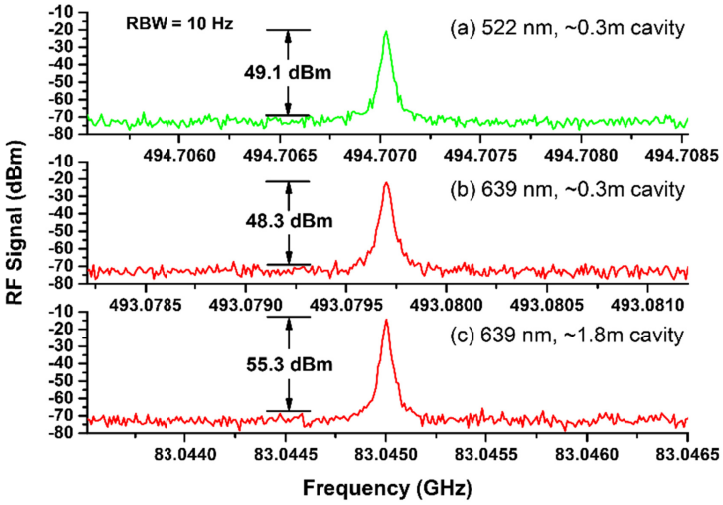

Fig. 6 Radio-frequency spectra of the self-mode-locked lasers operating at the wavelength of 522 nm and 639 nm with a cavity length of ~0.3 m ((a), (b)) and ~1.8 m ((c)) at a bandwidth of 3 kHz and resolution of 10 Hz.

It deserves noting that once the lasing threshold is reached by appropriately adjusting the laser cavity, the laser system steps into a stable mode-locked operation instantaneously, with no need of any mechanical perturbation. The locking mechanism is presumed to be the Kerr effect. Bai et al. [9] proposed a novel self-mode-locking mechanism in narrowband lasers based on the analysis of the gain-line splitting induced by an intra-cavity laser field. The model of the self-started Kerr-lens mode-locking consists of a laser gain media and an intensity modulator. The laser gain media can be thought of as an amplifier that has a gain line shape, which can be modeled by a frequency filter. As for the amplifier, the saturation effect should also be taken into account and its effect on the gain factor g is given as

$$g = \frac{g_{ss}}{1 + P/P_{sat}}, \tag{1}$$

Where g_{ss} is the small-signal gain factor, P is the signal power, P_{sat} is the saturation power. With regard to the gain line shape, Pr:YLF laser is solid-state laser with a gain-line shape corresponds to Lorentzian profile which belongs to homogeneous broadening [8]. The gain coefficient can be expressed as

$$g(\nu) = g(\nu_0) \cdot \frac{\Delta\nu/(2\pi)}{(\Delta\nu/2)^2 + (\nu - \nu_0)^2}, \tag{2}$$

among which ν_0 is the central frequency and $\Delta\nu$ is Full Width at Half Maximum (FWHM) of the laser gain-line shape. For the $^3P_0 \rightarrow {}^3F_2$ transition line at 640 nm, $\Delta\lambda$ is 0.69 nm, leading to a $\Delta\nu$ of 506.2 GHz. Owing to the spatial-temporal narrowing of the signal by Kerr-lensing effects of the gain media, the intensity of the intracavity laser is modulated passively. The model of the intensity modulation can be briefly thought of as a Gaussian profile in the time domain and be written as

$$\mathrm{IntMod} = e^{-\ln 2 \times \left(\frac{t - t_0}{\Delta t / 2}\right)^2}, \tag{3}$$

where t_0 is the reference time, and Δt is the FWHM of the modulation signal. After the laser crystal, the signal propagates in the atmosphere, where it experiences no chromatic dispersion or nonlinear effect, and is governed by the linear differential equation

$$\frac{\partial A}{\partial z} + \frac{L}{2} A = 0, \tag{4}$$

where L is the cavity round-trip loss, and can be solved by using the finite element method. After one round trip, the signal is fed in the gain media again and completes another round trip. The process is repeated until equilibrium is reached.

The simulation results that coincide with the FWHM of the measured spectrum depicted in Fig.7 (b), which was 0.39 nm, is depicted in Fig. 7(a) and 7(b). In this simulation, the FWHM of the modulation signal Δt was tuned to 3.5 ps so that the FWHM of the calculated spectrum was also 0.39 nm. As is shown in Fig. 7(a), a stable optical pulse was obtained with a pulse width of 1.5 ps, leading to a time-bandwidth product of 0.427, meaning a transform limited result. As a comparison, simulations with no intensity modulation was also carried out, the response in time domain and the simulated wavelength are illustrated in Fig. 7(c) and 7(d), respectively. As can be seen, the result in the time domain becomes a direct current signal, and the FWHM of the simulated wavelength was shortened, corresponding to a continuous-wave operation state.

It is interesting to note that, in our experiments, when the laser was mode-locked, laser spectrums with a relatively big dip in the center shown as the red line in Fig. 8(b) were sometimes captured. The possible reason for the dip in the laser spectrum is the frequency shift caused by gain-line splitting [9]. By introducing a frequency shift of the Stark splitting Δv_s from the unperturbed frequency induced by the intra-cavity laser field, Eq. (2) can be written as

$$g(\nu) = \frac{1}{2} g(\nu_0) \cdot \left[\frac{\Delta\nu/(2\pi)}{(\Delta\nu/2)^2 + (\nu - \nu_0 - \Delta\nu_s)^2} + \frac{\Delta\nu/(2\pi)}{(\Delta\nu/2)^2 + (\nu - \nu_0 + \Delta\nu_s)^2} \right], \tag{5}$$

By substituting Eq. (5) into the system instead of Eq. (2) and adjusting the frequency shift Δv_s to 176 GHz (corresponding to a wavelength of 0.16 nm) and modulation duration in Eq. (3) to 45 ps, we can obtain a simulated spectrum almost identical to the registered one shown as the red line in Figure 8(b), with a FWHM of 0.39 nm. As shown in Figure 8(a), the FWHM of the corresponding optical pulse was 2.4 ps, resulting in a time-bandwidth product of 0.936. It should be noted that, to get the simulation results, the duration of intensity modulation model raised almost 13 times compared with the case without frequency shift resulted from gain line splitting, which reveals the fact that the stark shift has the effect of modulating intensity, or in another word, compressing optical pulses. This conclusion is consistent with the experimental results reported by J. J. Sanchez-Mondragon in 1986 [10].

The frequency shift of the gain line stark splitting was once considered as the cause of self-start mode locking [9]. As shown in the green line in Figure 8(b), the amount of frequency shift in our case (Δv_s to 176 GHz, Δv of 506 GHz) already meets the requirements for the rough self-mode-locking criterion $12\Delta v_s^2 > \Delta v^2$ of solid-state lasers. For verification of the origin of self-start mode locking, we removed the intensity modulator and made the same simulation; the results are shown in Fig. 8(c) and 8(d). As can be seen, frequency shift caused by gain line splitting would induce fluctuations of transient laser power in the time domain, but it alone cannot give rise to stable ultra-short pulses with a period of the cavity round-trip time without the help of intensity modulation, which might be caused by Kerr-lensing effect.

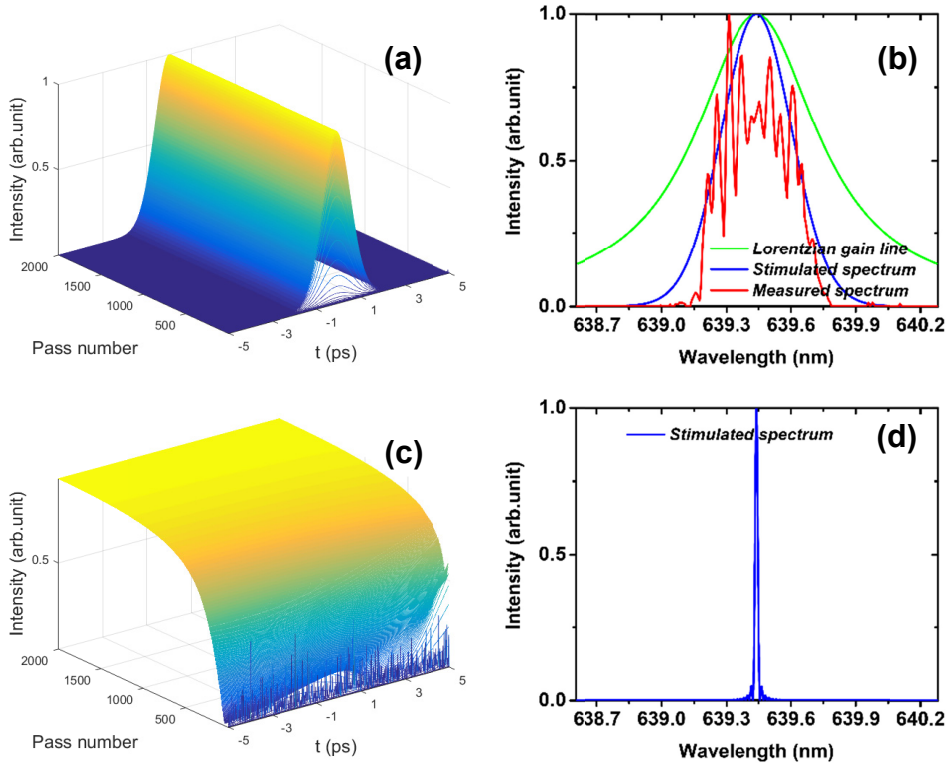

Fig 7. Simulated pulse evolution and final spectrum without frequency shift caused by gain line splitting. (a) and (b) are the situations with intensity modulation; (c) and (d) are situations without intensity modulation.

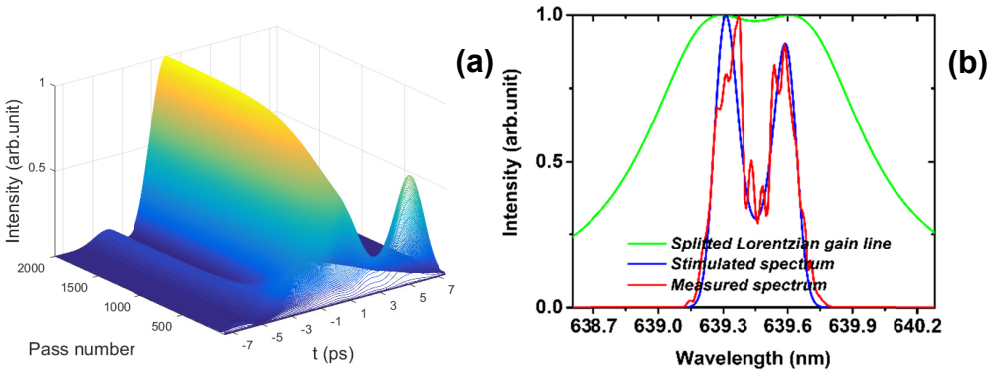

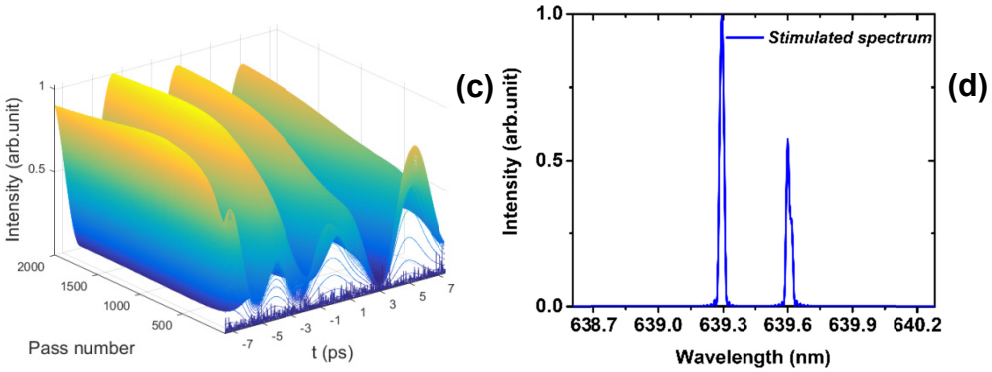

Fig 8. Simulated pulse evolution and final spectrum with frequency shift caused by gain line splitting. (a) and (b) are the situations with intensity modulation; (c) and (d) are situations without intensity modulation.

4. Conclusion

In this paper, efficient tens and hundreds of MHz self-mode-locked green and red lasers in a Pr:YLF crystal with three-mirror and six-mirror cavities using a double-end-diode-pumped structure without the need of any additional components was demonstrated. Thanks to the double-end pumped scheme, with an absorbed pump power of ~2.8 W, more than 0.68 W average output power operating in the cw mode locked state with a slop efficiency of 29.9% with respect to the absorbed pump power for 522 nm green laser and more than 1.44 W with a slop efficiency of 57.3% for 639 nm red laser were obtained. The output pulse trains and power spectrums demonstrate steady mode-locked operations at the maximum output power for hours. The spectral width (FWHM) of the 639 nm self-mode-locked operation with an effective cavity length of 1.61 m was measured to be 0.39 nm. Theoretical analysis was conducted to illustrate that the mode-locking mechanism was mainly due to the intensity modulation caused by Kerr-lensing effect and the gain line splitting dose make mode-locking easier but also broadens the pulse width.

5. Funding and Acknowledgments

National Natural Science Foundation of China (61275050, 61575164)